Degradation of structural safety levels in prototype balanced beam systems

Degradation of structural safety levels in prototype balanced beam systems

Rosario Ceravolo[1,2*], Erica Lenticchia[1,2], Gaetano Miraglia[1,2], Valerio Oliva[1,2]

[1]Department of Structural, Geotechnical and Building Engineering,
Politecnico di Torino, Corso Duca degli Abruzzi 24, 10129 Torino, Italy.

[2]Responsible, Risk, Resilience interdepartmental Centre (R3C),
Politecnico di Torino, Corso Duca degli Abruzzi 24, 10129 Torino, Italy.

Abstract

Post-tensioned balanced beam structures are very sensitive to natural deterioration and excessive environmental attacks, which can lead to relatively rapid drops in safety levels. Since partial failure or corrosion of pre-stressing tendons can be difficult to detect, the strategy of last resort to ensure that safety levels are acceptable remains to perform a mechanical load test, with the risks that this entails. In the case of some iconic balanced beam systems, destructive investigations are further limited by the need to comply with the deontological standards valid for cultural heritage structures. The capacity and robustness of balanced beam systems can therefore be estimated by relying primarily on accurate mechanical models and sensitivity analyses against scenarios that may degrade safety. To this end, reference models can be corroborated by information from various sources, including experimental campaigns and archives. This study, in particular, focuses on the evaluation of the residual capacity offered by Morandi's prototype balanced beam scheme, to aid prognosis, and possibly support "decision-making" for possible reuse. Finally, an experimental and numerical application to the most complex post-tensioned concrete balanced beam system ever designed by Riccardo Morandi is presented, i.e. the roofing system of Pavilion V of Torino Esposizioni dating back to the late 1950s.

KEYWORDS: (Safety assessment, Balanced beam, Progressive collapse, 20th Century architectural heritage, Riccardo Morandi, Experimental test campaign, Model calibration)

1. INTRODUCTION

Structural schemes in which pre-stressed tendons represent the main load-bearing elements are found in many concrete structural typologies. Iconic examples are undoubtedly the balanced beam schemes introduced by Riccardo Morandi and associated with post-tensioned concrete techniques [1]. Given the essential function of post-tension for the purposes of static equilibrium, the deterioration problems due to corrosion and other adverse phenomena raise serious concerns about the long-term durability of post-tensioned systems, with possible sudden and fatal consequences in these types of structures [2] [3] [4] [5]. This is particularly true for early post-tensioned systems, for which problems of corrosion may be accelerated by the poor-quality materials and poor construction practices such as inadequate duct venting, incomplete duct filling strands congestion, or poor consistency with segregation, poor maintenance [6], etc. On the other hand, 20th century heritage structures present specific issues, connected to the materials and techniques used for the construction, as well as to the complex and innovative spatial solutions; the continuous experimentations in all these areas have been among the characteristic features of architectural and engineering research of the past century.

Although in-depth checks on the state of pre-compression would be necessary in order to adapt modern heritage structures to current safety standards, the extensive use of experimental investigations clashes with compliance with the deontological standards relating to listed buildings [7] [8]. For these reasons, minimally invasive experimental techniques and accurate modeling must be favored for the evaluation of structural performance, with regards to safety levels in both static and seismic conditions.

The experimental activities aimed at identifying the structural characteristics are fundamental to determining the state of health of these structures or predicting the response to accidental actions. A number of experimental and numerical studies have been conducted on this topic. In many of these the corrosion of pre-stressed concrete beams and the loss of pre-stress have been investigated through changes in the properties such as stiffness and ductility or vibration response such as natural frequencies and mode shapes [9] [10] [11] [12] [13]. In others, magnetic flux leakage, radiography,

guided ultrasonic waves and acoustic emission techniques have been used [14] [15] [16] [17] [18]. Although each of these techniques has its advantages and disadvantages depending on the specific case, it is necessary to consider the clear difficulties in determining the residual pre-stress force and the level of corrosion in each single cable of a structure.

Another critical aspect in the structural assessment procedure for reuse is the progressive evolution of safety standards over the years. In fact, safety verification based on the application of current standards on the designer's original simplified models invariably leads to insufficient safety levels. A possible solution is to recur to updated models to match the experimental results as closely as possible in terms of mechanical properties, measured displacements or other identified parameters [6] [19].

In light of the concepts set out above, monitoring activities play a fundamental role, both in structural reassessment and conservation processes. Indeed, monitoring is not only a method to investigate the past of the structure, but it can play an active role in the conservation of heritage buildings and influence decision making. After the collapse of Polcevera Viaduct by Morandi the scientific community has once again stressed the paramount role of maintenance and continuous structural health monitoring (SHM). This is particularly true for prototype balanced beams conceived and built in an era when regulations were limited and poorly detailed on some aspects, such as the durability of concrete structures and design provisions to ensure robustness against progressive collapse [8].

The purpose of this work is to study the progressive deterioration of the safety levels of prototypes of balanced beam systems, also for the purposes of their reuse, with the aim of defining a minimally destructive diagnostic approach for these iconic structures. To this end, the research must necessarily leverage scenario-driven sensitivity analyses conducted on experimentally validated models. In fact, sensitivity analyses with respect to both corrosion and stress loss scenarios in the pre-stressing strands are of great practical use in the condition assessment of early post-tensioned systems, especially when it is not possible to carry out exhaustive experimental checks [20].

In order to demonstrate the scenario-driven approach, this article reports some significant results obtained on the safety assessment of Morandi's hypogeum Pavilion V in Torino Esposizioni, Turin, Italy.

The paper is structured as follows. Section 2 introduces the balanced beam scheme and its use for bridges and roofing systems. In Section 3, general issues with the structural assessment of prototype structures such as balanced beams are discussed. Section 4 presents the execution and the results of the experimental tests conducted on a balanced beam system. Section 5 deals with the safety assessment of Morandi's balanced beam with respect to progressive collapse for static loads, while Section 6 extends the study to the intertwined balanced beam scheme used by Morandi for the underground pavilion of Torino Esposizioni. Finally, Section 7 draws some conclusions on the degradation of safety levels of balanced beam systems and on the consequent diagnostic approach.

2. PROTOTYPE BALANCED BEAM SCHEME

The balanced beam scheme with subtended tie rods is used in large span structures, such as bridges and large roofing systems, to reduce the bending moment at midspan. This scheme can produce important economic savings for the amount of material used. In fact, both the height of the ribs and the number of cables needed are reduced, compared to the beam with simply supported scheme. Morandi's prototype balanced beam scheme has lateral cantilevers, which provide a first reduction of bending moment in the span. Furthermore, the scheme with subtended tie rods (or post-tensioned shorter strut beams) acquires greater efficacy accentuating the cantilever effect, thanks to the application of a concentrated load at the end of the cantilevers and to the use of inclined inwards longer strut beams (capable of naturally providing an additional axial compression component to the rib).

The load applied to the cantilevers by tensioning balances the maximum and minimum bending moments to achieve the most efficient configuration. **Figure 1** shows the bending moment diagrams for different static schemes of the beam, considering a uniformly distributed load.

A wide range of formal solutions and dimensional ratios between the resistant sections of various parts of the structure can be obtained considering the different inclinations attributable to the longer strut beams and the induction of pre-stressing force both in the ribs and in the terminal tie-rods (or shorter strut beams).

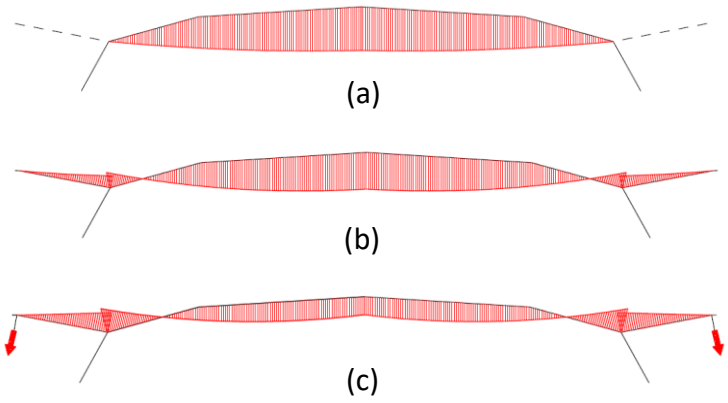

Figure 1 Qualitative comparison of the bending moment between support beam (a), balanced beam with lateral cantilevers (b), and balanced beam with subtended tie rods (c).

Various structures were conceived and built by Morandi with balanced beam scheme [21], [1]: the bridge over the Cerami in Enna (1953-1954), the overpass of the Via Olimpica in Rome (1958-1959), the bridge over the Vella in Sulmona (1960-1962) and finally the underground Pavilion V of Torino Esposizioni Center (1958-1959). In the case of the bridge over the Cerami, the first to be built with this methodology, it can be observed that the minimum vertical encumbrance of the beams was obtained by subjecting the terminal tie rods to a pretension capable of induce a useful moment in the span to compensate the moment of the beam considered in a simply supported scheme. The tie rods are made of high strength steel, inside fibre cement sheaths.

Subsequent works, such as the Via Olimpica overpass in Rome (**Figure 2**), represent the culmination of the most advanced solutions with balanced beam with in which Morandi express the whole theory of pre-stress technique.

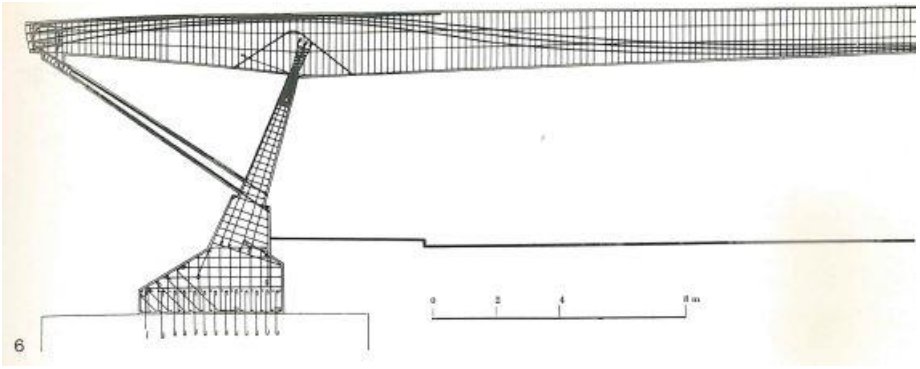

Figure 2 Via Olimpica overpass, Rome, 1958-1959: longitudinal half section [22].

Pavilion V was built in 1959 by Riccardo Morandi, commissioned by Società Torino Esposizioni, almost entirely owned by the FIAT motor company, to expand the existing exhibition spaces dedicated to hosting the Automobile Shows, also in view of the celebrations of 100 years from the unity of Italy, in 1961 [1]. The project became an opportunity for Morandi to take advantage of his prototype balanced beam scheme, widely used by the designer between the 1950s and 1960s in bridges and overpasses [21]. The pavilion consists of a single wide space, 69 m in width and 151 m in length, located 8 m below ground level (**Figure 3**).

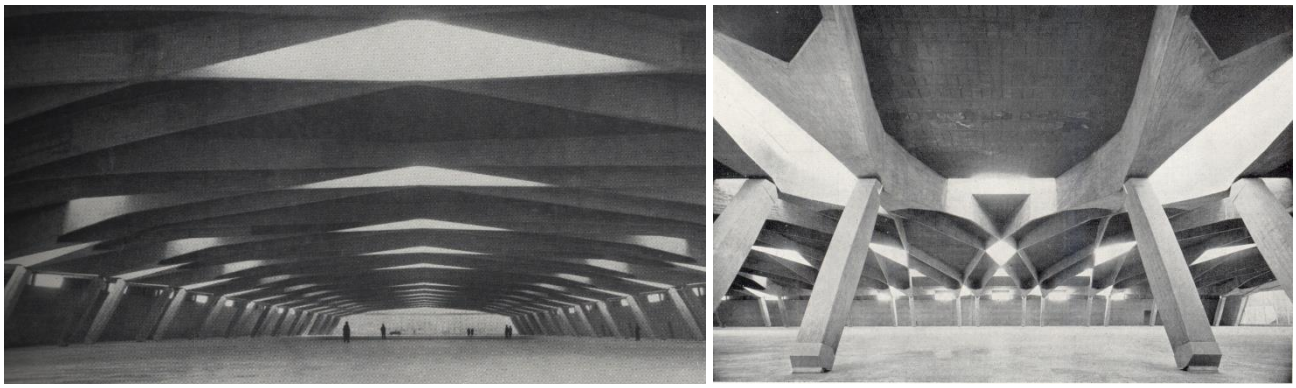

Figure 3 Underground Pavilion V in Torino Esposizioni by Riccardo Morandi: general views.

The structural scheme is composed of post-tensioned beams on two inclined supports, with two cantilevering side spans subsequently anchored by post-tensioning tendons at their ends, exerting a balancing effect on the bending moments in the main span. Unlike the usual bridge scheme, in Pavilion V the main post-tensioned ribs are not parallel beams but are diagonally directed and multiply

reciprocally interconnected to obtain a spatial structure offering high overall rigidity and lateral stability and to contrast the instability of the very thin webs (16 cm) of the main ribs. Furthermore, the post-tensioned ties at the ends of the lateral spans of the ribs are not inclined tendons anchored on the foundations of the main inclined supports, as in the bridges by Morandi, but are short ties embedded in prestressed concrete prismatic elements (shorter strut beams, located above the retaining walls), whose tension forces are balanced by the lateral retaining walls and by the load of the soil acting on their foundations.

In the case of Pavilion V, the shorter strut beams follow the inclination (even if not parallel) of the internal longer ones (**Figure 4**). The elements were conceived with the aim of transforming the static scheme from determined to undetermined. The internal inclined strut beams represent the other support for the entire structure. These elements have a hexagonal shape, tapering from the centre to the two ends to perform the hinge constraint at the extremity points. At the top of these elements, the steel plates provide the connection with the ribs. The steel plates allow the rotation with respect to the vertical plan, ideally creating an element capable of supporting actions only along its axis but unable to absorb bending moments.

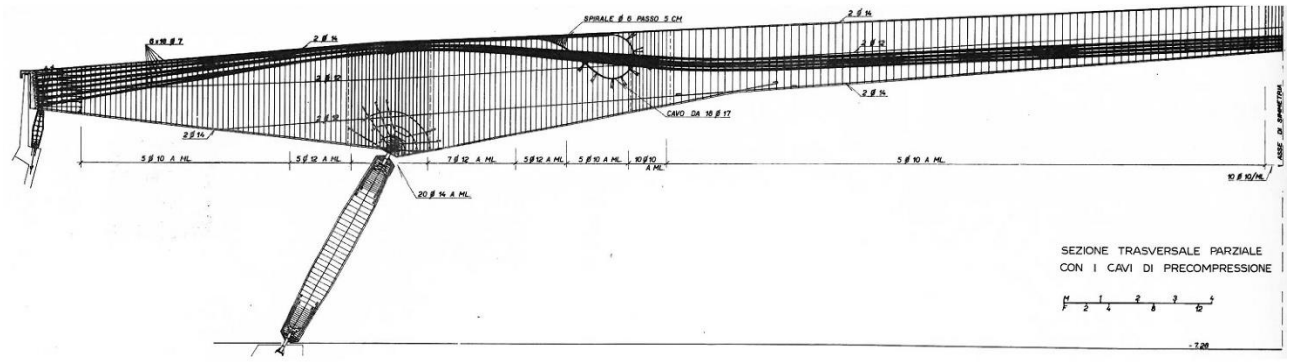

Figure 4 Post-tensioning cables of the Pavilion V balanced beam (half section) from a drawing in Morandi's documents [23].

3. ISSUES WITH THE SAFETY ASSESSMENT OF PROTOTYPE STRUCTURES

The design of new types of construction in the past was often based on physical models, which can represent complex behaviours, especially when they are reproduced on a scale very close to the actual one [24] [21]. On the contrary, even if numerical models can become fallacious when applied to systems with complex behaviors, they prove effective in solving problems in which, within the limits of instrumental or computational approximations, theory finds a good correspondence with real observation. Numerical tools in general are also cheap and lend themselves to generalizations.

One of the main issues in the safety evaluation of prototype structures, such as the balanced beam, is that there are no standards for their modeling. However, an advantage of numerical models is that they can be corroborated at any time to become realistic, because reality is continuously evolving and so do experimental measurements, since the system, as well as the surrounding environment, undergo changes. Therefore, a numerical model is typically able to assimilate new information [25].

Continuous or periodic monitoring activities can detect changes in the system properties or surrounding environment. If this change is small, periodic (e.g., daily or seasonal), and persistent, it is said to be physiological. If assimilating the system's physiological behaviors into the model is important, incorporating pathological behaviors is fundamental. Pathological behavior typically corresponds to a permanent or temporary change in an environmental condition that produces a permanent change in structural properties. If such pathological behaviors occur, they must be taken into account in the models by updating the constitutive laws of the materials or even geometric and topologic properties. In the end, this approach leads to a sort of digital twin of the structure, where experimental data are released as a part of an ongoing updating and condition assessment process.

ICOMOS standards point to the importance of periodic controls of the construction as the primary tool for the preservation of architectural heritage [7] [26] [27]. Usually, the inspections of buildings, useful to improve the knowledge level and reduce the uncertainties, can be executed on a one-off basis or periodically, and most observations and measurement methods supply only local information.

Modern SHM techniques, which are typically applied to inspect the global structural behavior, try to overcome the limitations of traditional and visual inspections [28]. Vibration-based SHM has been successfully used for damage detection and quantification in existing structures. Dynamic tests provide information about the whole-body response and allow extending to the whole structure the outcomes of the local inspections and measures. These techniques are particularly useful in the architectural heritage field because of their usual non-invasiveness and non-destructiveness and because they provide direct information about the dynamic response and indirect information about structural integrity [7] [25]. Moreover, the dynamic test setups can be easily installed and removed.

In the light of their advantages, vibration-based SHM techniques are particularly suitable to understand the dynamic response of complex structural systems, such as the one represented by 20th century architectural heritage, which not only present specific issues, connected to their complex and innovative spatiality, but are also characterized by the continuous experimentations of designers and engineers in the use of materials and technologies as specific features of this heritage [29].

In these as in other reinforced concrete buildings, infill walls and expansion joints may strongly affect the dynamic behavior of the structure and, consequently, should be accounted for accurate numerical reproduction [8]. For all these reasons, the results of the numerical analysis need to be reconciled with: i) historical information and survey documentation; ii) experimental data (coming from both vibration-based techniques and classical mechanical test) [30], [31].

Contrary to traditional architectural heritage, for 20th century heritage a large number of documents of various nature are available; in fact, the calculation assumptions and models of safety employed by the designers are often available, as well as safety levels prefigured at the time of their construction. Under these conditions, the experimental corroboration of a model offers indications on the possible decay of safety margins and allows for “a posteriori” evaluations in the Bayesian sense.

As stated in Section 1, being able to rely on an updated model is of great importance in the safety condition assessment of balanced beam systems.

3.1. Post-tensioned systems

Post-tensioned systems, including balanced beams, generally require an extended and systematic program of inspections and diagnostic investigations to be performed as the basis for the subsequent analyses and evaluations in the possible strengthening design stage, in terms of assessments of durability and residual service life, and of structural safety and reliability. Investigations will necessarily include traditional physical–chemical tests aimed at determining the strength of the materials, the geometric characteristics, grouting defects, carbonation front, steel corrosion and other chemical attacks [32].

Post-tensioning evaluations are generally difficult on systems with internal tendons. In addition, global dynamic characteristics are virtually insensitive to variations in internal stresses. Indeed, vibration-based SHM is not used to directly detect broken reinforcement, but rather to guide local non-destructive methods to be used in cascade. In these cases the local tests of choice are endoscopies or radiographies.

Among the usual diagnostic objectives for reinforced and pre-stressed concrete structures, the inspection and diagnostic investigations sometimes must face challenging problems: for instance, accurately diagnosing corrosion or detecting grouting defects in post-tensioned cables in remote positions. Even greater criticalities are found when investigating the durability structural elements constructed with materials, technologies and patents that have not seen a great diffusion.

In consideration of the problems outlined above, and specifically in balanced beams, the models cannot realistically take into account any corrosion or tension losses in the reinforcements, except in terms of carrying out sensitivity analyses with respect to the presence of defects in the internal tendons.

4. EXPERIMENTAL INVESTIGATIONS ON BALANCED BEAMS

Reusing 20th century concrete architectures entails the challenge to guarantee new extended service life to concrete structures built many decades ago and face the need for a seismic assessment in compliance with new standards and with reference to the local seismic risk reports. Although in-depth analysis and investigations on some of these iconic structures were recently carried out, only in few cases this has led to targeted and extensive experimental campaigns, e.g. [8] [30] [33].

To investigate the experimental behavior of the balanced beam scheme, reference will be made to the most complex realization by Morandi among those previously mentioned, namely Pavilion V in Torino Esposizioni, for which it was possible to carry out a complete cognitive and diagnostic process. Indeed, in 2019 Pavilion V was subjected to a broad range test campaign by Politecnico di Torino [34] [35], since a full structural condition assessment was deemed necessary for a possible reuse as part of the university campus of architecture.

Figure 5 (left) reports the model of the pavilion with detailed geometric information, which allowed for appropriate understanding of the structural characteristics of the pavilion and the recognition of possible design and construction principles. The structure is divided into three main bodies by means of two expansion joints, which cross the roof and the external walls (**Figure 5** center), and whose behavior was uncertain. Based on the geometric model, a preliminary elastic FE model was also created.

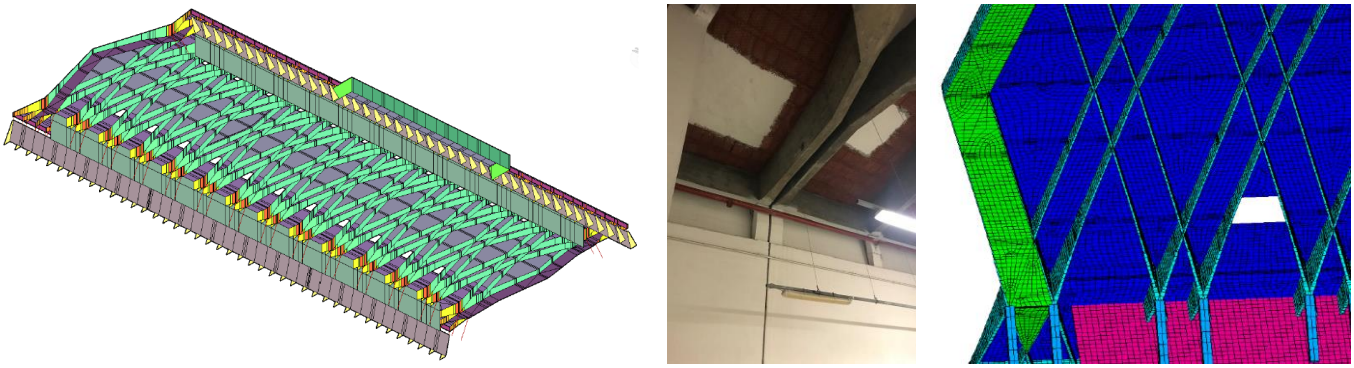

Figure 5 Pavilion V: geometric model (left), expansion joint detail (center) and detail of the FE model at the ribs (right).

In the 2019 campaign, both destructive and non–destructive tests were performed (see **Figure 6**) [34]. Among other things, inspections on the structures were carried out to determine the concrete cover, layout and characteristics of post-tensioning cables, possible grouting defects, steel corrosion and other chemical attacks, and geometric characteristics in terms of position and diameters of reinforcing bars (pacometric investigations). Moreover, a direct check was carried out for each element type through a scarification, while rebound hammer tests were performed to verify the homogeneity of the mechanical characteristics of the concrete.

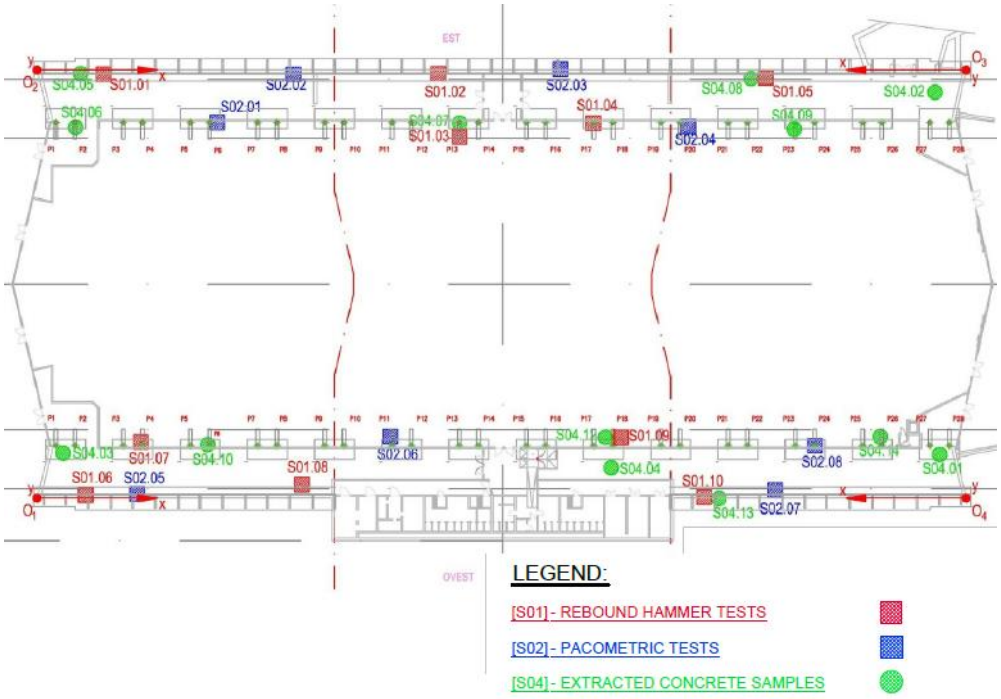

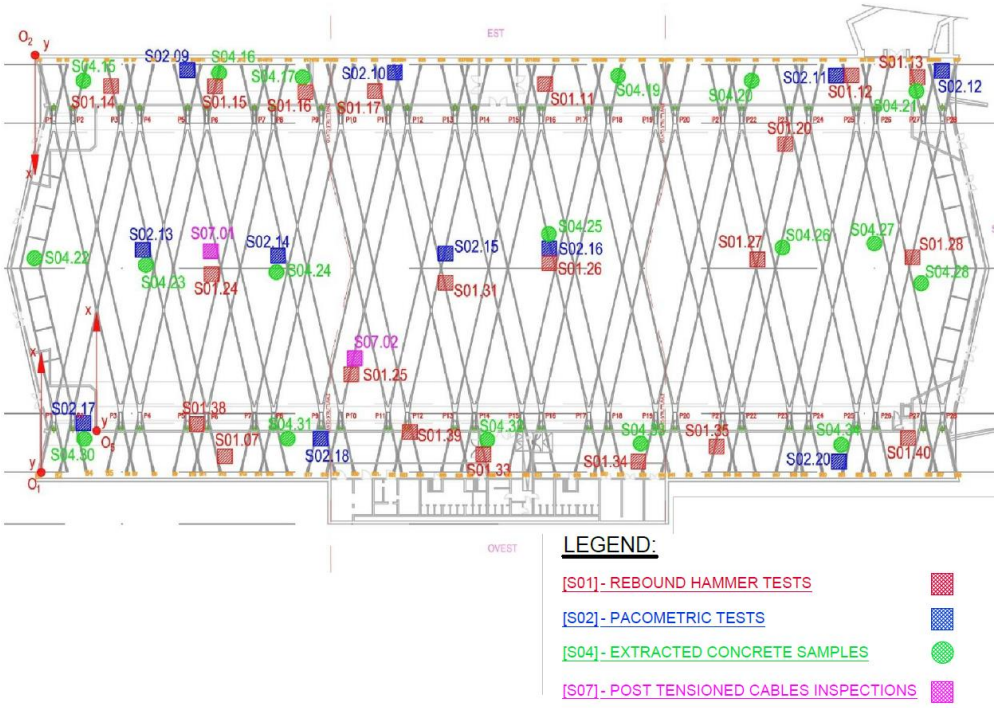

Figure 6 Pavilion V: test positions at the underground floor (above) and at the roof level (below) [34].

The following paragraphs describe respectively the mechanical and load tests, the dynamic tests, and the investigations on the pre-stressing system.

4.1 Mechanical tests

Mechanical tests have been executed to evaluate the compressive strength of the different elements of the structure: samples were extracted from foundations, retaining walls, ribs, and longer strut beams (see **Figure 7** left). Each sample was analyzed with phenolphthalein to determine the progression of the carbonation front (**Figure 7** center) and then subjected to a compression test. The specimens were extracted and tested according to UNI EN 12504-1:2009 [36] and UNI EN 12390-3:2009 [37]. The total number of specimens extracted and tested was 32 [34]. **Table 1** summarizes the depth, diameters, ratios depth/diameter, compressive strengths, and carbonation depths of the cores.

Table 1 Results of concrete compression tests: average depth *h*, average diameter *d*, ratio *h/d*, ultimate load *F*, compressive strength f_c and average carbonation depth *c* [34].

SPECIMENS	***h* (mm)**	***d* (mm)**	***h/d* (-)**	***F* (kN)**	**f_c (MPa)**	***c* (mm)**
S04-01 (Foundations)	107.32	104.35	1.03	278.1	32.5	0
S04-02-A (Foundations)	116.36	104.23	1.12	253.2	29.7	0
S04-02-B (Foundations)	110.82	104.25	1.06	170.6	20.0	0
S04-03 (Foundations)	213.28	104.26	2.05	273.7	32.1	0
S04-04 (Foundations)	218.34	104.35	2.09	493.2	57.7	0
S04-05 (Retaining walls)	215.53	104.40	2.06	398.7	46.6	10
S04-08 (Retaining walls)	110.03	104.32	1.05	538.9	63.0	10
S04-13 (Retaining walls)	109.54	104.33	1.05	523.3	61.2	10
S04-06 (Longer strut beams)	194.82	93.80	2.08	407.9	59.0	3
S04-07 (Longer strut beams)	198.17	93.80	2.11	248.6	36.0	20
S04-09 (Longer strut beams)	194.54	93.90	2.07	363.3	52.5	4
S04-10 (Longer strut beams)	194.57	93.75	2.08	459.9	66.6	5
S04-12 (Longer strut beams)	194.94	93.73	2.08	341.0	49.4	5
S04-14 (Longer strut beams)	105.84	93.76	1.13	290.0	42.0	15
S04-15 (Ribs)	115.37	104.38	1.11	328.0	38.3	45/-
S04-16 (Ribs)	113.77	104.40	1.09	217.3	25.4	70/70
S04-17 (Ribs)	102.08	104.40	0.98	529.6	61.9	20/25
S04-19 (Ribs)	98.67	93.93	1.05	351.2	50.7	27/-
S04-20 (Ribs)	101.00	93.86	1.08	277.6	40.1	30/-
S04-21 (Ribs)	184.86	93.91	1.97	259.3	37.4	25/20
S04-22 (Ribs)	101.69	93.91	1.08	223.8	32.3	40/40
S04-23 (Ribs)	99.42	93.91	1.06	329.0	47.5	30/20
S04-24 (Ribs)	103.99	93.84	1.11	237.1	34.3	40/40
S04-25 (Ribs)	102.52	93.86	1.09	293.3	42.4	35/35
S04-26 (Ribs)	100.98	93.83	1.08	260.6	37.7	35/30
S04-27 (Ribs)	104.50	93.87	1.11	212.7	30.7	45/40
S04-28 (Ribs)	97.57	93.90	1.04	317.0	45.8	45/40
S04-30 (Ribs)	195.49	93.95	2.08	277.0	40.0	35/30
S04-31 (Ribs)	193.17	93.92	2.06	259.2	37.4	35/25
S04-32 (Ribs)	98.22	93.95	1.05	334.4	48.2	-/20
S04-33 (Ribs)	99.67	93.93	1.06	277.7	40.1	30/-
S04-34 (Ribs)	98.42	93.87	1.05	330.0	47.7	20/-

These results show that the structure is made of concrete with reasonably high compressive strength. Different strength values can be ascribed to distinct causes. The higher values in the retaining walls

could be due to humidity conditions that could have influenced the hardening of concrete. Furthermore, the carbonation levels of most samples are relatively low.

Figure 7 Pavilion V: Extraction of a concrete sample from a longer strut beam (left); carbonation tests on the samples of the ribs (center); view of the static tests with trucks connected to the ribs through jacks (right) [34].

The testing campaign also included static load tests on two different ribs, to assess the bearing capacity of the structure under the characteristic combination of actions (see **Figure 7** right). The load tests have been carried out using 7 hydraulic jacks with a maximum capacity of 100 kN, connected in parallel to an hand pump equipped with a pressure sensor and a load cell. Each jack has been connected to the structure by means of a steel chain, passed through a hole made in the rib (maximum diameter of 80mm and position determined following both pacometric and endoscopic inspection aimed at avoid interference with cables and reinforcements), and contrasted by fully loaded three-axle trucks (approximately 300kN). Displacement potentiometric transducers (novotechnik, model TR0050) have been used for the measurement of the displacements. The normalized vertical displacements progressively measured during the test on a rib are reported in **Figure 8**. At the end of each loading phase, the displacement measures stabilization has been checked before proceeding with the next increase or decrease. The forces measured by the load cell are to be considered as applied equally at each loading points. The measurement points for displacements have been located adjacent to the loading points and also in correspondence of adjacent ribs to evaluate the transversal collaboration [34].

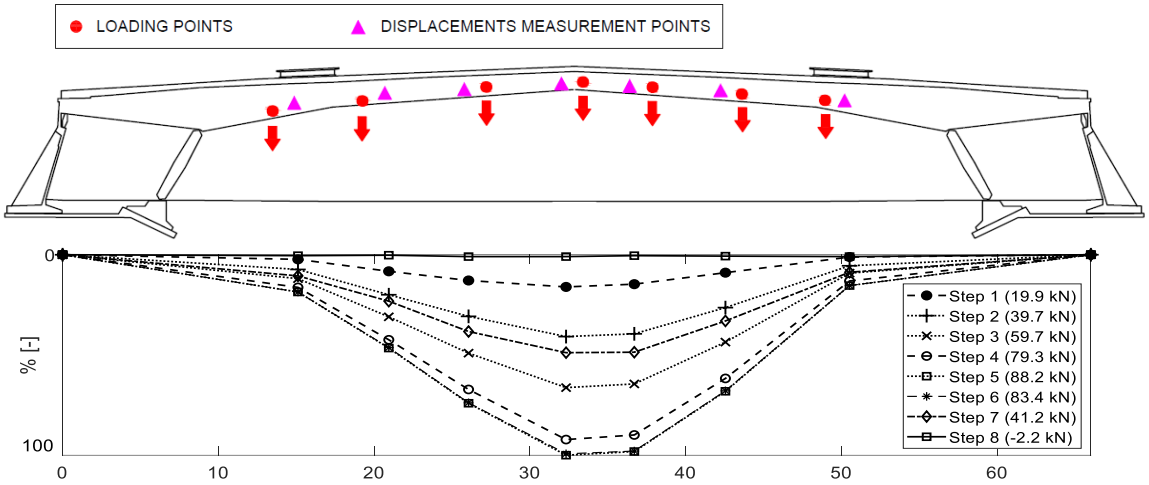

Figure 8 Pavilion V: normalized vertical displacements measured during the static test on a rib [34].

The maximum displacement measured during the static test on a rib was 4.36 mm. This result showed a relatively high stiffness of the structure under the imposed loads, despite a span of approximately 48 m between the inner supports. Moreover, the small displacements have proven a significant transversal collaboration of the ribs due to the numerous intersections between these elements, confirmed by the displacement measurement on the adjacent rib (equal to 3.20 mm in Step 5).

4.2 Dynamic tests

Ambient vibration measurements were performed to identify the modal characteristics, reconstruct the global dynamic behavior of the pavilion, and highlight possible criticalities in the seismic response [35], [38].

The structural complexity of Pavilion V directly affects the dynamic behavior of the building and the design of a successful design of the dynamic tests setup [39], [33]. A non-negligible source of complexity is due to the great rigidity of the system, as well as its interaction with the ground and the non-structural inner walls made of cellular concrete. Further uncertainties are related to the dynamic behavior of the expansion joints. In this case, the preliminary FE model of the pavilion played a fundamental role in designing the acquisition setups.

The acquisition system was composed of 20 monoaxial piezoelectric accelerometers (PCB Piezotronics, model 3701G3FA3G, sensitivity 1 V/g, Frequency Range 0 to 100 Hz, Resonant Frequency ≥400 Hz, Overload Limit ±3000 g pk, Temperature Range −40 to +185 °F), positioned on the ribs, struts and rods. Overall, two setups were designed, paying close attention to favoring the modal decoupling. The first configuration was designed to obtain information in the horizontal (x-y) plane, while the second one mainly focuses on the vertical direction (**Figure 9**) [38].

The red arrows in **Figure 9** represent the horizontal channels of the accelerometers. The latter were indicated adding an "x" symbol inside the circle when a vertical channel is also considered. Whereas, the blue circles indicate accelerometers with only a vertical channel.

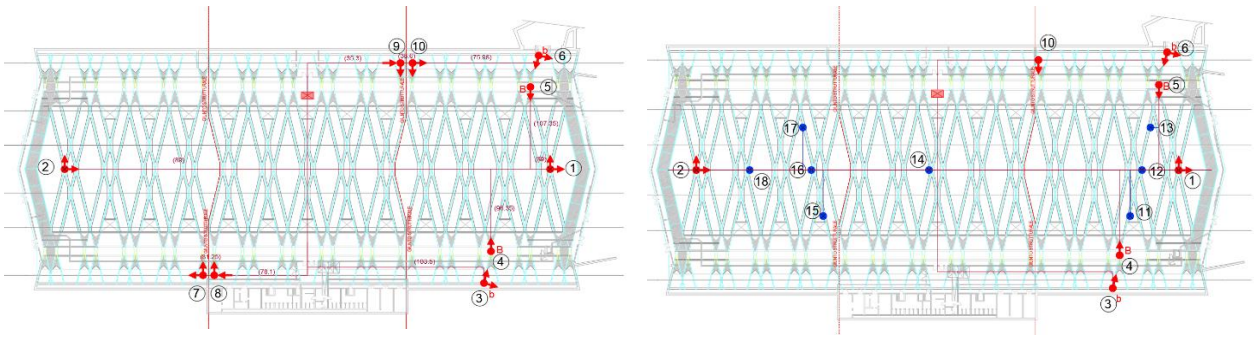

Figure 9 Accelerometers configurations: setup 1 (left) and setup 2 (right) [38].

The dynamic tests were conducted on the 18 and 19 February 2019. The signals acquired correspond to the structure response to environmental noise excitation, produced by external stochastic forces such as wind and vehicular traffic. The acquisitions lasted between 18 and 98 minutes. The signals, in terms of accelerations, were sampled at 128 Hz and 256 Hz for setup 1 and setup 2, respectively, as the main modes were confined in the first 20 Hz [8], [38].

The modal parameters were estimated from a data processing procedure that includes an output-only system identification algorithm of the Stochastic Subspace Identification (SSI) family. In particular, the third algorithm considered by the unifying theorem of Van Overschee and De Moor, known as "Canonical Variate Analysis" (CVA), was implemented [40] [41]. A cluster analysis has been used to group the possible physical modes into homogeneous sets representing the same physical mode.

Among the different types of clustering analysis, the agglomerative hierarchical clustering has been implemented in the code [42]. The most recurrent experimental mode was seen to be the one at 2.57 Hz. By way of example, the stabilization and clustering diagrams of the identification of a sub-signal are reported in **Figure 10**.

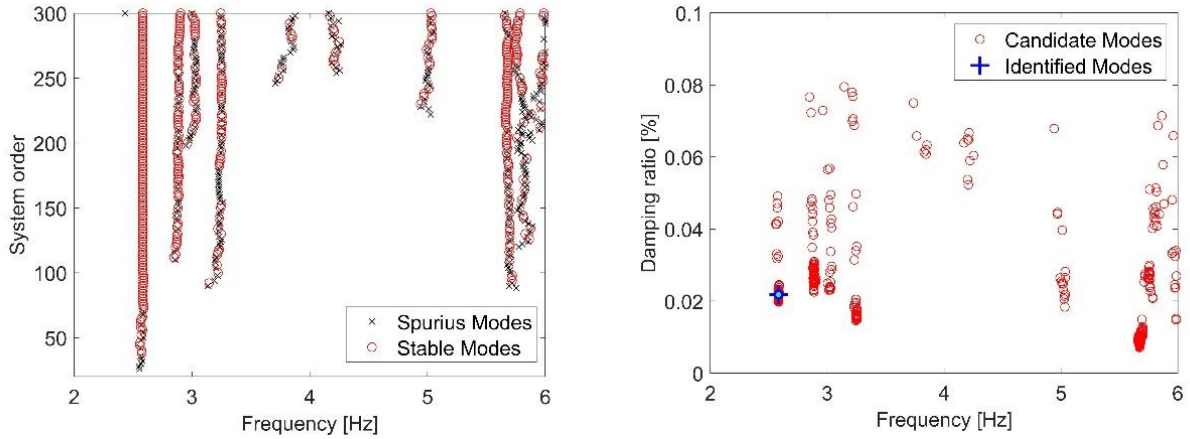

(a) (b)

Figure 10 Stabilization (a) and clustering (b) diagram of the identification performed on the sixth sub-signal of setup 1 of the entire Pavilion V, with evidence of the mode at 2.57 Hz [39].

Table 2 reports the comparison between the experimental frequencies identified on the channels associated with each of the three blocks and verified on the preliminary FE model. **Table 3**, in turn, shows the same comparison in terms of equivalent viscous damping. The most evident finding, resulting from the ambient vibration-based tests, is the substantial effectiveness of the two joints, as demonstrated by the appearance of distinct modes for each of the three blocks (in this regard the reader is referred to [39]).

Table 2 Comparison between the frequencies (f_{EXP}) identified for the three blocks of the pavilion.

		NORTH BLOCK	***CENTRAL BLOCK***	***SOUTH BLOCK***
Mode	**Description**	f_{EXP} **(Hz)**	f_{EXP} **(Hz)**	f_{EXP} **(Hz)**
1	mainly horizontal mode	2.57	2.57	2.57
2	mainly vertical mode	2.68	2.73	2.73
3	mainly horizontal mode	5.72	5.67	5.72

Table 3 Comparison between the damping (ζ_{EXP}) identified for the three blocks of the pavilion.

		NORTH BLOCK	***CENTRAL BLOCK***	***SOUTH BLOCK***
Mode	**Description**	$\boldsymbol{\zeta_{EXP}}$**(%)**	$\boldsymbol{\zeta_{EXP}}$**(%)**	$\boldsymbol{\zeta_{EXP}}$**(%)**
1	mainly horizontal mode	2.11	2.11	1.90
2	mainly vertical mode	0.98	2.36	1.38
3	mainly horizontal mode	0.80	4.18	0.70

4.3 Investigations on post-tensioning tendons

Partial rupture or corrosion of post-tensioning tendons are difficult to directly locate using non-destructive tests, even if some high damping values found in translational modes have directed investigations towards local checks on the post-tensioned system of some sample balanced beams (locations S07.01 and S07.02 in **Figure 6**). In fact, despite the impossibility of making an exhaustive program of endoscopies and local assays, the inspections on the tendons of two ribs have revealed: i) presence of corrosion or full-blown rupture of some wires in the tendons, ii) poor grouting; iii) positioning errors. The poor grouting allowed to carry out an endoscopy inspection inside the duct (**Figure 11**).

In particular, hardened gray grout was found along the lower portion of the ducts, while poor segregated grout was found at the upper portion of the tendon, probably due to gravity separation processes. The grout filling of the ducts was not complete and regions where grout was segregated exhibited air voids along the top of the duct.

Grout contamination by Cl^-, which facilitates corrosion when in exceeding concentrations [3] [43], have not been investigated. However, regions of different grout quality and presence of strand corrosion products, which can affect the durability of the elements, were visually assessed.

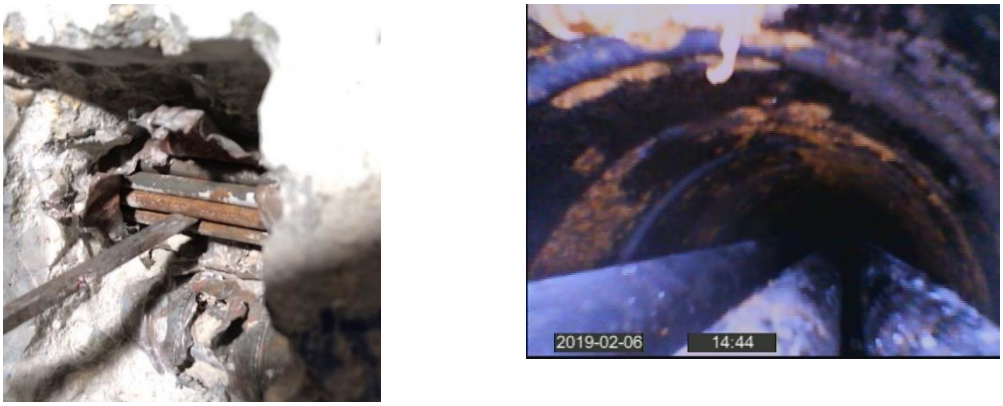

Figure 11 Visual inspection of post-tensioning tendons in the ribs at location S07.01 (left), and endoscopy inspection inside a duct of the rib at location S07.02, where grout filling of the duct is seen to be incomplete (right) [34].

5. STRUCTURAL REASSESSMENT AND SAFETY DEGRADATION IN THE BALANCED BEAM

From the analysis of the original documentation consisting of executive drawings and the calculation reports of Pavilion V [23], it was possible to identify the typical static scheme used by Morandi for the balanced beam scheme, as shown in **Figure 12**.

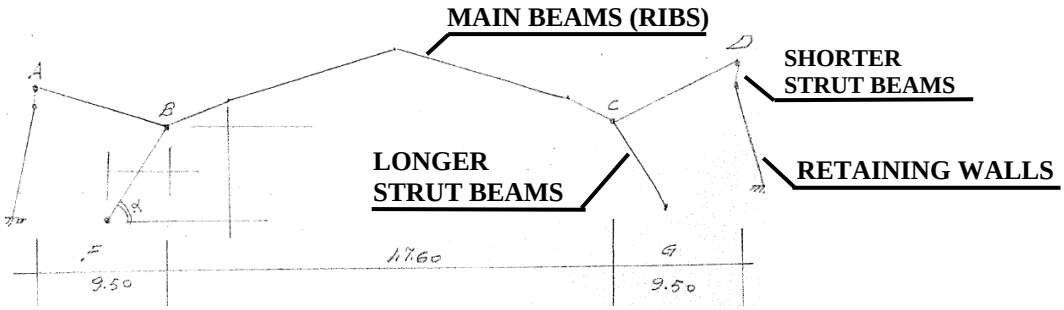

Figure 12 The static scheme of the balanced beam from a sketch inside Morandi's calculation report of Pavilion V [23].

In the calculation report, the geometric characteristics of different segments of the rib, the weights of the various segments, the permanent loads, the weight of the filling soil acting on the extrados of the roof, and finally, the imposed crowd load on the roof (equal to 4 kN/m^2) were defined.

For the permanent loads Morandi assumed a static scheme in which the constraints in A and D were not present because the shorter strut beams were not connected to the ribs in the initial stage of the construction process. Subsequently, he introduced the action of the shorter strut beams placed in A and D in order to reduce the positive bending moment at midspan. Finally, with the delayed constraints in A and D present on the ribs, he introduced the crowd loads on the roof. Among the various configurations, Morandi also considered the behavior for the structure subjected to thermal expansion, which generates a variation in the bending moments. At worst, an increase of the moment due to thermal effects was estimated in the order of 1%. Another effect concerns the obliquity of the frames since an inclination angle of 13° with respect to the transverse axis affects the span of the rib. As a whole, the deviation in the bending moments was summarized by the simple ratio of the spans (1.025), which Morandi included in the approximation of the calculation.

In Morandi's documentation, the maximum permissible stresses are reported for the materials used in the pavilion. For the foundation, concrete with cubic strength at 28 days of 15 MPa was used, 35 MPa for the retaining walls and 45 MPa for the shorter, longer strut beams and ribs. Regular Aq 50 reinforcement bars were used in the structure, with yield strength no less than 270 MPa. Regular reinforcing bars in Italy have nowadays a nominal yield strength of 450 MPa (B450C steel [44]), thus about 66% greater than that one used by Morandi at that time. Finally, special steel was employed for pre-stressing cables with a diameter of 7 mm and rupture stress of 1750 MPa.

As shown in **Figure 4** with a symmetrical half section from the original drawing, in each balanced beam, four long cables have been positioned longitudinally that cross the entire rib and two short cables for each of the two lateral cantilevers. Moreover, vertical cables have been placed into the shorter strut beams to apply a concentrated downward load at the edges. The process of tensioning these elements was based on a series of successive operations: once the construction was completed and after the hardening of all the resistant parts, and with the shorter strut beams free from the ribs, the following steps were carried out: i) tensioning of the four long cables at 600 MPa; compensation for an equal

intensity from the opposite extremity; filling with soil above the roof; ii) tensioning of the short longitudinal cables at 1150 MPa; dismantling of formwork outside the longer strut beams; iii) tensioning of the vertical cables at 289 MPa; iv) tensioning from one end to 1150 MPa of the longitudinal cables (second tensioning); compensation for an equal intensity of the opposite edge; total dismantling of the formworks; locking of the connection of short strut beams with plates; v) tensioning of the vertical cables at 315 MPa; recalibration and grouting of injection mortar inside the sheaths [23]. The structural reassessment of the post-tensioned rib of Morandi's original scheme has been carried out according to Eurocode 2 (EC2) [45] at different stages: a) design stage, in accordance with the values reported by Morandi; b) design stage, based on the compression strength of samples taken during construction, following the values reported in the test certificates issued in 1959 by the official lab of the Politecnico di Torino [46] (hereinafter referred to as *REASS 1959*); c) after 60 years, in accordance with the strength values reported in the test certificates issued in 2019 by the same lab.

Regarding concrete strength, the plots in **Figure 13** refer to the samples tested in 2019, and correspond to the prior and posterior probability and cumulative density functions for compression strength, f_c, obtained from Bayesian updating formulations [47], [48]. In particular, the density functions of both probability and cumulative (posterior PDF and CDF) have been calibrated on 18 samples extracted from the ribs and then tested.

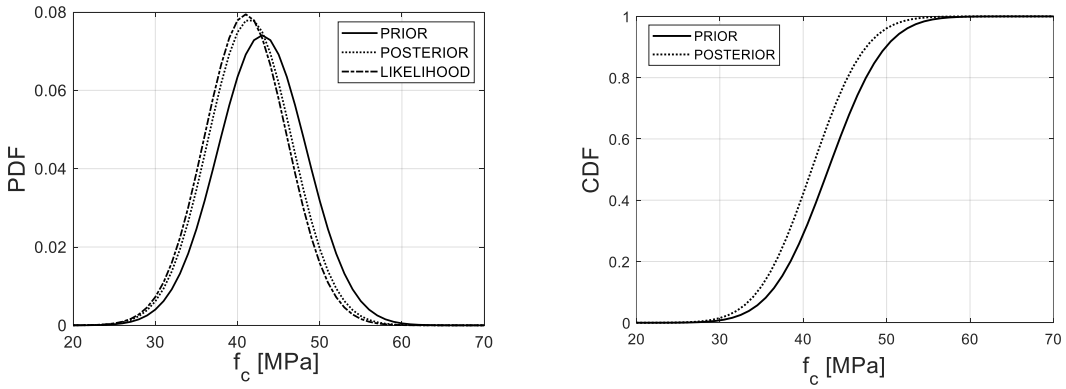

Figure 13 Concrete compression strength in a post-tensioned rib of Pavilion V as a results of 2019 campaign: prior and posterior probability density function (PDF) (left) and cumulative density function (CDF) (right).

The Bayesian updating results in a decrease of the average concrete compression strength of the ribs from 43.00 MPa to 41.51 MPa. As reported in the following subsection, this decrease on material strength (approximately 3÷4%) leads to a reduction of the ultimate load multiplier on the rib from 1.55 to 1.40 (approximately 10%), considering the cables in good health state.

5.1 Crowd load multipliers

Morandi's results are reported in **Figure 14**, where the bending moment diagrams of the rib refer to permanent loads (b), post-tensioning of the shorter strut beams (c), and imposed crowd loads (d), respectively. According to the original calculations, the diagrams take into account the vertical offset between the rib axis and the hinge of the longer strut beam, which amounts to 1.47 m (**Figure 14** a).

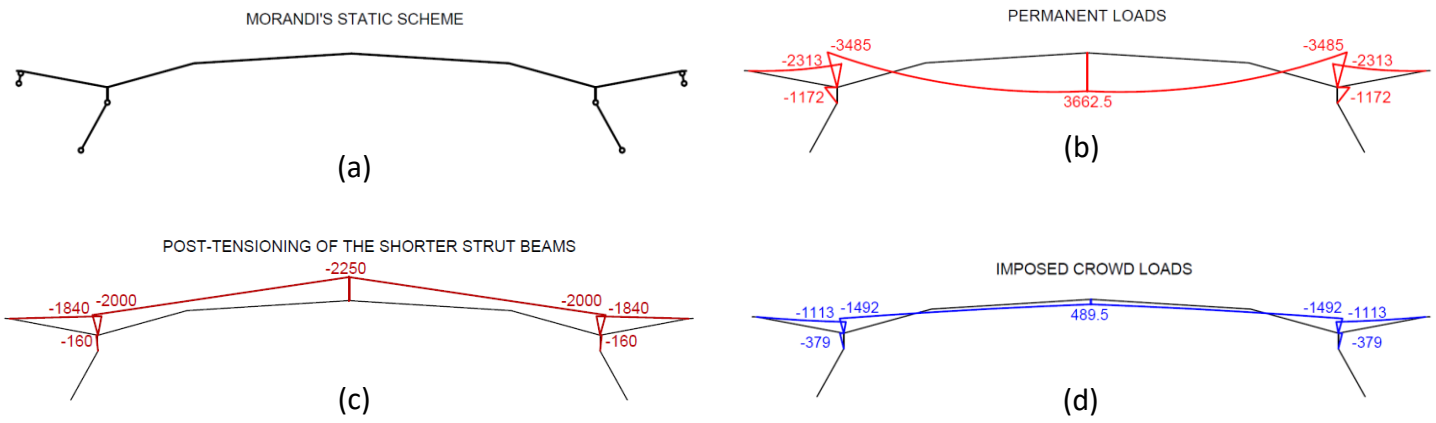

Figure 14 Scheme with vertical offset from Morandi's calculation report (a) and bending moment (kNm) acting on a rib as resulting from Morandi's scheme; (b) due to the permanent loads; (c) due to post-tensioning effect of the shorter strut beams; (d) due to the imposed crowd loads [23].

In full consistency with these schemes, **Table 4** contains a comparison between the ultimate load multipliers (for bending moment verification at midspan and at the supports) calculated with the design values of concrete strength and those resulting from the posterior values for the ribs. In particular, ultimate load multipliers $\alpha = q_{Rd}/q_d$ were defined as the ratio between the ultimate crowd load on the roof with respect to a specific verification, q_{Rd}, and the imposed load, q_d. Accordingly, these multipliers were calculated: i) at the design stage with the regulation in force at the time [49] using nominal values

of actions and strengths (Regio Decreto - *RD39* [49]), ii) at the design stage with the current standards (Eurocodes - *EC* [50], [45]), iii) at a reassessment stage with the compression strengths evaluated on samples taken during construction (with the current standards) (*REASS 1959*), and iv) at a reassessment stage with the posterior values resulting from the tests conducted in 2019 (with the current standards) (*REASS* 2019, [44], [34]). It is worth highlighting that Morandi assumed a crowd load, q_d, equal to 4 kN/m^2 (imposed load in **Figure 14** d).

Table 4 Comparison between ultimate load multipliers calculated: at the design stage (*RD39*); at the design stage with the current standards (*EC*); at the reassessment stage during construction (*REASS 1959*); at the reassessment stage in 2019 (*REASS 2019*). μ and σ represent the mean and standard deviation assumed for the concrete compression strength.

	RD39	***EC***	***REASS 1959***	***REASS 2019***
μ_{fcm} (MPa)	-	43.00	42.17	41.51
σ_{fcm} (MPa)	-	5.38	5.08	5.10
α_{midspan} (-)	1.68	1.55	1.47	1.40
α_{supports} (-)	4.04	4.77	4.74	4.71

From **Table 4** it can be noted that at the supports the load multipliers are greater than at midspan. Moreover, the previous results show that, as regards concrete, the updated load multipliers approximately remain in line with Morandi's original project. However, as reported in Section 6, the inspections on the tendons of two ribs have revealed some broken wires in the tendons, together with poor grouting and positioning errors. According to [13], the sensitive parameters should be assessed in real-time, and for particular loading conditions, to evaluate the possible trends induced by pre-stress steel losses or corrosion. The direct inspections focused on two ribs of the roof located in two different blocks and they investigated one point of a single cable. These two inspections aim to reach a preliminary and localized knowledge on post-tensioned cables corrosion state. Direct inspections prove reliable and objective, but they have the disadvantage to provide only local information. An inspection campaign aimed at reaching an exhaustive level of knowledge for the corrosion level is

required to probabilistically estimate the actual safety levels of the whole post-tensioned systems, in order to obtain more expressive results for decision-making on possible reuse. However, while numerous other tests were carried out on this iconic building, deontological standards did not permit direct investigations of the post-tensioned cables in an exhaustive manner for the entire structural system. Consequently, the condition assessment has been conducted in terms of sensitivity analysis with respect to the percent reduction of the post-tensioning steel area, as well as to the errors in positioning the cables and at this stage is limited to a single typological rib.

5.2 Degradation of structural safety as a function of post-tensioning area loss

The sensitivity analysis concerned the parameters A_r (area of the post-tensioning tendons) and d_p (effective depth of the cross-section) of the resistant section, which constitute the main terms used by the designer to calculate the bending moment capacity. In particular, these analyses were performed considering the coupled axial force and bending moment verification with reference to the ribs under direct investigation, i.e. S07.01 (**Figure 6**). Referring to the structural scheme of the simple balanced beam (**Figure 14** a), it has been assumed at this stage that wire corrosion (and error in positioning) increases uniformly. Accordingly, the plots in **Figure 15** report the ultimate load multipliers at midspan as a function of the assumed corrosion in the wires of the ribs and the positioning error (in percent of effective depth) referring to the cables centroid, respectively. **Figure 16**, in turn, report the same quantities at the supports. At midspan, referring to Morandi's documents, the centroid was at 105.5 cm with respect to the extrados of the rib (with an overall depth of 130 cm). Thus, in **Figure 15** b, 10% error means an error of approximately 10.5 cm, which corresponds to the position of the centroid at 95 cm. At the supports the centroid was at 272.5 cm with respect to the intrados of the rib (with an overall depth of 292 cm). Thus, in **Figure 16** b, 10% error means an error of approximately 27 cm, which corresponds to the position of the centroid at 245.5 cm.

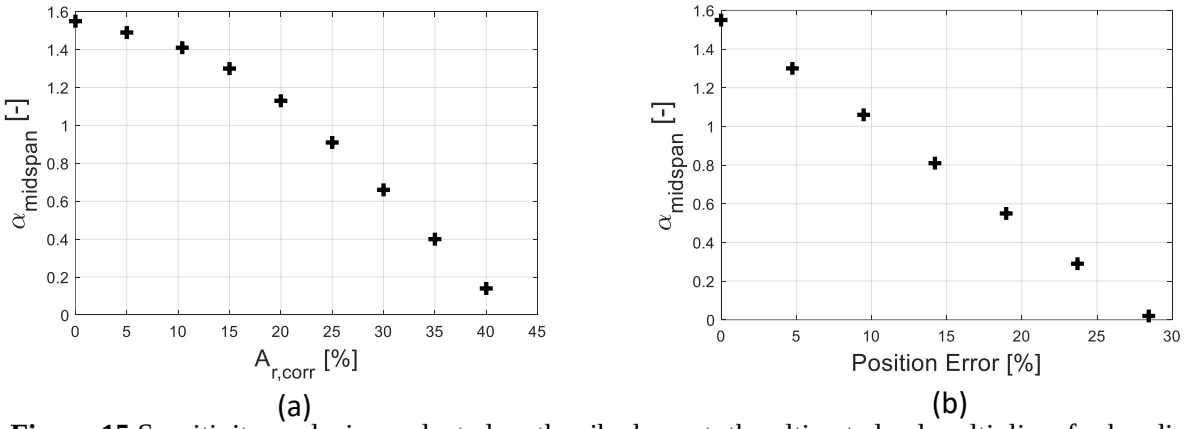

Figure 15 Sensitivity analysis conducted on the rib element: the ultimate load multipliers for bending moment verification at midspan on Morandi's scheme as a function of loss of post-tensioning steel area in the rib (a) and of the positioning error (in percent of the effective depth) of tendons (b).

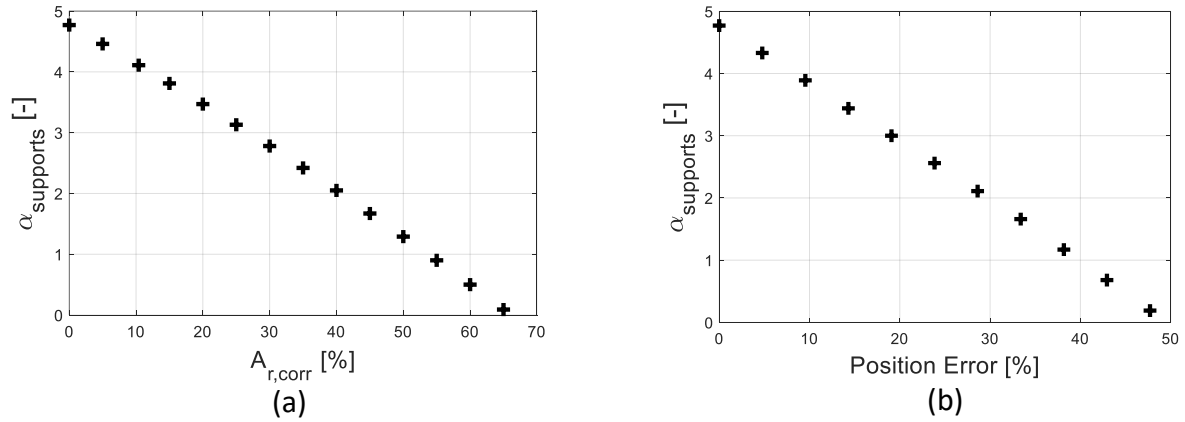

Figure 16 Sensitivity analysis conducted on the rib element: the ultimate load multipliers for bending moment verification at the supports on Morandi's scheme as a function of corroded post-tensioning steel area in the rib (a) and of the positioning error (in percent of the effective depth) of tendons (b).

Additionally, a sensitivity analysis has been conducted for the condition assessment concerning also the reduction of post-tensioning steel area of the shorter strut beam elements. The corrosion in these elements causes an increase of bending moment in the middle of the rib and a reduction (in terms of absolute value) of bending moment at the supports. **Figure 17** reports the ultimate load multipliers (with respect to bending moment verification at midspan) as a function of the assumed corrosion in the wires both of the ribs and the shorter strut beams.

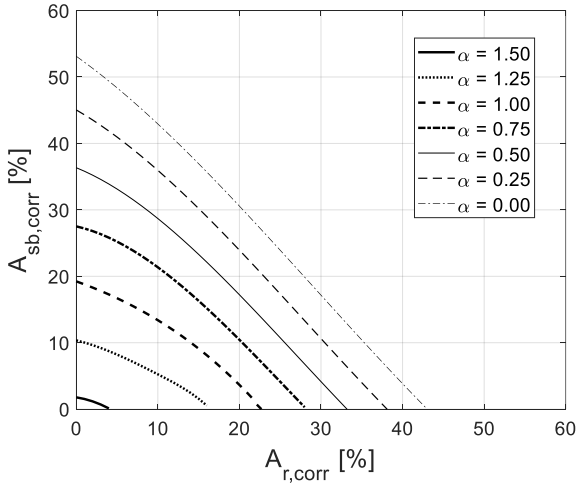

Figure 17 Sensitivity analysis conducted at midspan of the rib element: ultimate load multipliers on Morandi's scheme as a function of both loss of post-tensioning steel area in the rib ($A_{r,corr}$) and loss of post-tensioning steel area in the shorter strut beams ($A_{sb,corr}$).

6. STRUCTURAL REASSESSMENT AND SAFETY DEGRADATION IN THE INTERTWINED BALANCED BEAM

The baseline FE model of Pavilion V, created for a previous seismic assessment according to current standards [44], is mostly made of shell and beam elements used to represent the macro-elements composing the structure. In particular, the shorter and the longer strut beams were modelled with Timoshenko beams while for the roof, the ribs, and the retaining walls, Mindlin-Reissner shell elements were used [51]. The values of elastic moduli were initially assumed to be equal to those obtained from mechanical tests, in particular for the elements detailed in **Table 5** (ribs, retaining walls and longer strut beams).

Table 5 Values of the elastic moduli as resulting from the mechanical tests.

ELEMENT	**Elastic moduli from mechanical characterization tests (GPa)**
Ribs	33.0
Retaining walls	37.0
Longer strut beams	32.0

A calibration of the model, based on identified modes, was then performed by recurring to standard local sensitivity model updating techniques (for details on the updating procedure used, see [25]) on a simplified model. In particular, based on the results of the dynamic tests, the stiffness of the two joints between the three blocks was assumed to be zero [52]. The deflections measured during static tests also contributed to updating the roof model. In fact, the inertial and elastic properties of the roof were adjusted in the FE model to fit vertical displacements in **Figure 8** and, at the same time, the main vertical modes. In particular, an increment of the density from 2500 kg/m^3 to 3500 kg/m^3 has been applied for the shell elements of the roof (with thickness variable between 25 cm and 45 cm) in order to simulate the permanent load acting on it as an overlying distributed mass. Whereas, the Young's modulus has been increased from 25 GPa to 39.9 GPa to simulate the equivalent stiffness of the roof, considering the layers positioned over the concrete slab: the concrete screed and the cement stabilized soil. Instead, for the shorter strut beams, the Young's modulus was initially imposed by literature, then, given the aging conditions in common with the ribs, the value was modified in accordance to the experimental value obtained for those elements, i.e., 33 GPa.

A typical Young's modulus, i.e., 3 GPa, has been assumed, according to *SIA266* regulations, for the non-structural inner walls made of cellular concrete. These elements were inserted in the 90s as fire walls in order to convert the structure from an exhibition hall to an underground parking. Since the high uncertainty of this parameter (that range approximately from 0.9 to 4 GPa in accordance to SIA266, based on the type of blocks), and given the lack of information on this material, the value was calibrated recurring to automatic FE model updating techniques [53] by fitting the first identified mode in terms of mode shape and natural frequency.

Table 6 reports the values of the parameters for which no data were available from mechanical tests (roof, shorter strut beams and non-structural walls).

Table 6 Values of the elastic moduli before and after the updating based on the results of the dynamic tests.

ELEMENT	Elastic moduli of the initial FE model (GPa)	Elastic moduli updated (GPa)

Roof	25.0	39.9
Shorter strut beams	30.0	33.0
Non-structural walls	3.0	2.12

Thanks to the calibration process, the model simulates as close as possible the actual behavior of the real structure. In particular, the MAC between the experimental and predicted mode by the calibrated FE model equal 0.86 (first mode), with a residual normalized error in frequency of 0.08%.

It is worth underlining that the presence of effective joints in the roof constitutes a factor of seismic vulnerability due to the possible pounding between the three distinct bodies. Pounding could be aggravated by the lack of edge beams at some sections of the joints. In a retrofitting project, the joints should be redesigned to guarantee an integral diaphragmatic behavior, also by means of shock transmission devices, and to regularize the global longitudinal and transverse behavior of the roof. Most importantly, any retrofitting interventions must consider that seismic action is mainly entrusted to the shorter strut beams, which were not conceived to withstand important horizontal shear actions.

6.1 Crowd load multipliers of the intertwined balanced beam system

The same steps developed in Section 5, based on the simplified calculation schemes used by Morandi, have been repeated using the FE model updated after the test campaign conducted in 2019. **Figure 18**, in particular, shows the bending moment diagrams due to permanent (a) and imposed (b) loads on a rib resulting from the updated FE model.

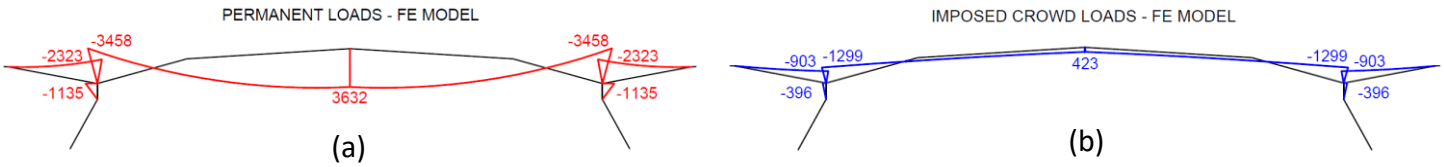

Figure 18 Bending moment diagrams on a rib resulting from the updated FE model: due to the permanent loads (a); due to the imposed crowd loads (b).

The comparison between **Figure 14** and **Figure 18** shows that the bending moments evaluated with the updated FE model are lower than the values obtained from simplified Morandi's schemes. In particular, at midspan the reduction in bending moments due to the permanents and crowd loads are approximately 1% and 13%, respectively. At the support, the same quantities are lower of approximately 0% and 18%.

As a consequence of the above, at the reassessment stage the sensitivity curves will undergo updating. The condition assessment results are shown in **Figure 19**, in terms of ultimate load multipliers α (with respect to bending moment verification at midspan) as a function of the loss of steel areas.

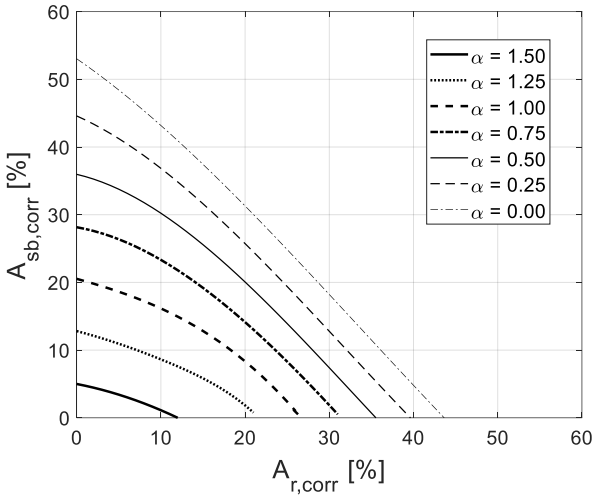

Figure 19 Sensitivity analysis conducted at midspan of the rib element with the calibrated FE model: ultimate load multipliers as a function of both loss of post-tensioning steel area in the rib ($A_{r,corr}$) and loss of post-tensioning steel area in the shorter strut beams ($A_{sb,corr}$).

The comparison between **Figure 17** and **Figure 19** shows that the load multipliers evaluated with the FE model are slightly higher than the values obtained from simplified Morandi's schemes. In fact, α increases from 1.40 (calculated with the updated concrete strength) to 1.65, considering the cables in good health state.

6.2 Degradation of structural safety as a function of post-tensioning area loss in the intertwined balanced beam system

In a subsequent condition reassessment stage, a portion of the structure made by the typological section (in transverse direction of the building) and a module by 11 m of depth (in longitudinal direction) has been analyzed. This portion of the building constitutes a system containing 4 interconnected ribs, 4 longer strut beams and 8 (4 pairs) shorter strut beams. On this system, which also corresponds to that used by Morandi for the loads analysis and the calculation of stresses in the structure, sensitivity analyses have been carried out considering the redistribution effect of the imposed crowd loads between the ribs. These analyses focused on the capacity of the main ribs.

The ultimate load multiplier of the analyzed portion of the structure has been evaluated (in each beam falling in this sub-system) following the models reported in EC2 [45] for prestressed reinforced concrete elements. In these models, the corrosion effect was considered by parametrically reducing the area of the pre-stressing cables. Then, to obtain a unique value of the ultimate load multiplier for the analyzed portion, α_{SYSTEM}, the average of the estimates obtained for the 4 ribs falling in this sub-system was used.

Figure 20 a reports the ultimate load multipliers of the rib system as a function of the assumed loss of steel area in the wires at midspan of the different ribs, $A_{r,corr,midspan}$, assuming absence of corrosion at the supports of the ribs. **Figure 20** b, in turn, reports the ultimate load multipliers of the rib system as a function of the assumed corrosion in the wires at the supports of the different ribs $A_{r,corr,support}$, assuming absence of corrosion at midspan. In this second case, the load multipliers of the rib system cannot in any case exceed the maximum value of 1.65 allowed by the bending moment capacity at midspan even in absence of corroded wires. In the case of combined corrosion condition at midspan ($A_{r,corr,midspan}$) and at the supports ($A_{r,corr,support}$) the ultimate load multiplier of the rib system is the minimum between the two single conditions.

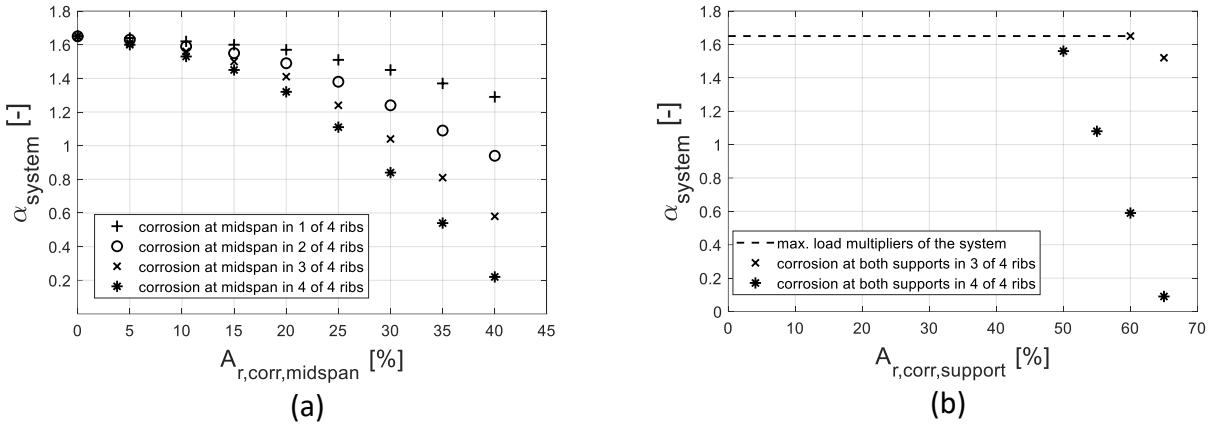

Figure 20 Sensitivity analysis conducted on the considered system composed of 4 ribs: ultimate load multipliers (for bending moment verification) with the updated FE model as a function of corroded post-tensioning steel area in the different ribs at midspan (a) and at the support (b).

As for the real stress distribution, it is worth underlining that also the viscoelastic effects due to the delayed restraint of the shorter strut beams (highlighted in subsection 3.1) should be investigated [54]. The results reported in **Figure 19** and **Figure 20** allows to understand how the safety margin level decreases in a single rib, and in the considered portion of the balanced beam system, with the progression of the strands corrosion, or in general with the decrease in prestressing force.

In the specific case of Pavilion V, loss in post-tensioning steel area, both in the midspan and at the support of the analysed system, would result in a significant decline of safety levels. However, the behaviour in the two situations is different, as observed in **Figure 20**: while loss of steel area in the midspan results in a gradual decrease of the ultimate load multiplier, the corrosion activated close to the support corresponds to a faster safety degradation. Initial safety margins, on the other hand, are much greater in the latter case, since a halving of the steel area at the support still allows the ultimate load multiplier remain at its maximum value, about 1.65 for the specific case study. Beyond that level of corrosion, however, safety degradation is ruled by corrosion at the support with rates that tend to double. It is therefore clear that the two collapse modes deserve very different types of monitoring. For instance static load tests can give useful indications on the current safety of the balanced beam, but only with respect to the corrosion in the midspan. Instead, a periodic monitoring program is

important to evaluate the corrosion rate in different parts of the post-tensioning system, especially near the supports.

7. CONCLUSIONS

This study concerned the progressive degradation of the safety levels of prototype balanced beam systems, also for the purposes of their reuse, with the aim of defining a minimally destructive diagnostic approach for such iconic structures.

The research made use of the only experimental campaign ever conducted on this structural system, i.e. the one which in 2019 had as its object Pavilion V of Torino Esposizioni. The campaign aimed to explore the behavior of the balanced beam, both as a single scheme and as a complex spatial system of intertwined beams, designed by Morandi to support the underground pavilion. The experimental results were exploited to corroborate first the model of the simple prototype beam and then the spatial system as a whole.

The updated models made it possible to verify that the safety levels of the system with supposedly efficient pre-tensioning steel are in line with what was predicted by the original calculations. However, the presence of damaged wires observed from a few endoscopies required scenario-based sensitivity analyses to be conducted on the models, also in order to comply with deontological standards for iconic or listed buildings. This allowed the construction of diagrams that estimate the degradation of safety levels as a function of the loss of post-tensioning steel area in different locations.

Simulations have shown that the loss of the post-tensioning steel area results in a significant drop in structural reliability, although the rates of reduction in safety levels are very different depending on the region in which the loss occurs. This means that static load tests, which currently represent the main tool for verifying complex prototype structures, do not provide sufficient information on the residual life of balanced beam systems.

In the case of Pavilion V, for high levels of corrosion, safety is no longer governed by the residual post-tensioning wires at the intrados, as per the original design calculations, but by those of the extrados near the support, which are the more subject to the action of rainwater and injection defects, following the formation of bubbles. It is also worth pointing out that tendons in the extrados position are the most difficult to inspect.

In conclusion, although the particular structural conception of Pavilion V, with the intertwining of ribs, makes it robust with respect to local weakening, progressive corrosion and defects in post-tensioning wires are confirmed to be the one of the main issue to be addressed for the preservation and reuse of balanced beam systems. A minimally destructive diagnostic approach, in addition to standard static load tests, should include periodical monitoring of corrosion or degradation rates, possibly extended to a suitable number of elements, in order to update the safety level estimates, thereby defining prognostic scenarios based on updated models.

With a view to an even more complete analysis, also the shear resistance of the individual members is an aspect to be explored, in consideration of the fact that the regulations of the time were very light and only provided a limitation on shear stresses, depending on the type of concrete and the presence or absence of a minimum reinforcement.

ACKNOWLEDGMENTS

The authors wish to thank the Materials and Structures testing lab (MASTRLAB) and in particular Dr. Antonino Quattrone. Test activities were developed under the general supervision of the building and logistics office of the Politecnico di Torino (EDILOG), led by Arch. Gianpiero Biscant. This article is dedicated to the memory of Professor Piero Marro, who has also provided valuable suggestions for this research.

REFERENCES

[1] E. Bruno, "Riccardo Morandi per il V padiglione di Torino Esposizioni," in *Olmo C., Pogacnik M., Sorace S., La concezione strutturale: Architettura e Ingegneria in Italia negli anni 50 e 60.*, Umberto Allemandi & C., Torino , 2013, pp. 229-240..

[2] L. Bertolini, B. Elsener, P. Pedeferri, E. Redaelli and R. B. Polder, Corrosion of Steel in Concrete: Prevention, Diagnosis, Repair, 2nd ed., Weinheim, Germany: Wiley-VCH, 2014.

[3] ACI222.2R-14, "Report on Corrosion of Prestressing Steels," *ACI Committee 222 Protection of Metals in Concrete against Corrosion*, 2014.

[4] *fib Model Code for Concrete Structures 2010,* fib 2013. Lausanne.

[5] Ministero delle Infrastrutture e dei Trasporti, Consiglio Superiore dei Lavori Pubblici, "Linee guida per la classificazione e gestione del rischio, la valutazione della sicurezza ed il monitoraggio dei ponti esistenti," Roma, Italy, 2020.

[6] W. Botte, E. Vereecken, L. Taerwe and R. Caspeele, "Assessment of posttensioned concrete beams from the 1940s: Large-scale load testing, numerical analysis and Bayesian assessment of prestressing losses," *Structural Concrete,* vol. 22, pp. 1500-1522, 2021.

[7] R. Ceravolo, G. De Lucia, E. Lenticchia and G. Miraglia, "Seismic Structural Monitoring of Cultural Heritage Structures," Springer, 2019, pp. 51-85.

[8] R. Ceravolo and E. Lenticchia, "Diagnosis and preservation of 20TH Century architectural Heritage: from the first thin shell solutions to the iconic structures built by Pier Luigi Nervi and Riccardo Morandi in Turin," in *7th Structural Engineers World Congress*, Istanbul, Turkey, 2019.

[9] J. T. Kim, Y. S. Ryu, H. M. Cho and N. Stubbs, "Damage identification in beam-type structures: frequency-based method vs mode-shape-based method," *Engineering structures,* vol. 25, no. 1, pp. 57-67, 2003.

[10] C. A. Jeyasehar and K. Sumangala, "Damage assessment of prestressed concrete beams using artificial neural network (ANN) approach," *Computers & structures,* vol. 84, no. 26-27, pp. 1709-1718, 2006.

[11] R. Capozucca, "Detection of damage due to corrosion in prestressed RC beams by static and dynamic tests," *Construction and Building Materials,* vol. 22, no. 5, pp. 738-746, 2008.

[12] S. Maas, A. Zürbes, D. Waldmann, M. Waltering, V. Bungard and G. De Roeck, "Damage assessment of concrete structures through dynamic testing methods. Part 1–Laboratory tests," *Engineering Structures,* vol. 34, pp. 351-362, 2012.

[13] M. P. Limongelli, D. Siegert, E. Merliot, J. Waeytens, F. Bourquin, R. Vidal and L. M. Cottineau, "Damage detection in a post tensioned concrete beam-Experimental investigation," *Engineering Structures,* vol. 128, pp. 15-25, 2016.

[14] A. Ghorbanpoor, R. Borchelt, M. Edwards and E. A. Salam, "Magnetic-Based NDE of Prestressed and Post-Tensioned Concrete Members: The MFL System," 2000.

[15] I. Bartoli, S. Salamone, R. Phillips, F. Lanza di Scalea and C. S. Sikorsky, "Use of interwire ultrasonic leakage to quantify loss of prestress in multiwire tendons," *Journal of Engineering Mechanics,* vol. 137, no. 5, pp. 324-333, 2011.

[16] A. Moustafa, E. D. Niri, A. Farhidzadeh and S. Salamone, "Corrosion monitoring of post-tensioned concrete structures using fractal analysis of guided ultrasonic waves," *Structural Control and Health Monitoring,* vol. 21, no. 3, pp. 438-448, 2014.

[17] B. H. Kim, "Evaluation of prestress force on bonded tendons using practical formula," *Experimental mechanics,* vol. 55, no. 2, pp. 439-447, 2015.

[18] A. Appalla, M. K. ElBatanouny, W. Velez and P. Ziehl, "Assessing corrosion damage in posttensioned concrete structures using acoustic emission," *Journal of Materials in Civil Engineering,* vol. 28, no. 2, p. 04015128, 2016.

[19] S. S. Law and J. Li, "Updating the reliability of a concrete bridge structure based on condition assessment with uncertainties," *Engineering Structures,* vol. 32, no. 1, pp. 286-296, 2010.

[20] B. Asgari, S. A. Osman and A. Adnan, "Sensitivity analysis of the influence of structural parameters on dynamic behaviour of highly redundant cable-stayed bridges," *Advances in Civil Engineering,* 2013.

[21] F. Levi and M. A. Chiorino, "Concrete in Italy. A review of a century of concrete progress in Italy, Part 1: Technique and architecture," *ACI Concrete Int.,* vol. 26, no. 9, pp. 55-61, 2004.

[22] G. Boaga, Riccardo Morandi, Bologna: Zanichelli, 1984.

[23] R. Morandi, *Sistemazione area del Galoppatoio in Torino. Calcoli di stabilità. Roma, 2 Aprile 1959.,* Archivio Maire Tecnimont, Torino, 1959.

[24] G. Oberti, "Le développement des essais sur modèles réduits de structures et l'exploitation des résultats," *IABSE publications,* vol. 26, pp. 345-363, 1966.

[25] R. Ceravolo, G. Pistone, L. Zanotti Fragonara, S. Massetto and G. Abbiati, "Vibration-based monitoring and diagnosis of cultural heritage: a methodological discussion in three examples," *International Journal of Architectural Heritage,* vol. 10, no. 4, pp. 375-395, 2016.

[26] ICOMOS, "Principles for the analysis, conservation and structural restoration of architectural heritage," 2003.

[27] ICOMOS International Committee on Twentieth Century Heritage (ISC20C), Approaches for The Conservation of Twentieth-Century Cultural Heritage, 2017.

[28] C. Farrar and K. Worden, "An introduction to structural health monitoring," *Phil. Trans. R. Soc. A,* vol. 15, no. 265, pp. 303-315, 2007.

[29] C. Croft, S. Macdonald and G. Ostergren, Concrete: Case Studies in Conservation Practice, Getty Publications , 2019.

[30] E. Lenticchia, G. Miraglia and R. Ceravolo, "Dynamic Identification of Large Thin Shell Structures in Concrete," in *13th International Conference on Structural Analysis of Historical Constructions SAHC 2023*, 2024.

[31] P. Pachón, M. Infantes, M. Cámara, V. Compán, E. García-Macías, M. Friswell and R. Castro-Triguero, "Evaluation of optimal sensor placement algorithms for the Structural Health Monitoring of architectural heritage. Application to the Monastery of San Jerónimo de Buenavista (Seville, Spain)," *Engineering Structures,* no. 202, 2020.

[32] D. Breysse, Non-destructive assessment of concrete structures: Reliability and limits of single and combined techniques: State-of-the-art report of the RILEM technical committee 207-INR, Vol. 1. Springer Science & Business Media, (Ed.) 2012.

[33] E. Lenticchia, G. Miraglia, A. Quattrone and R. Ceravolo, "Condition Assessment of an Early Thin Reinforced Concrete Vaulted System," *International Journal of Architectural Heritage,* vol. 17, no. 2, pp. 343-361, 2023.

[34] MASTRLAB, DISEG, "Prove di caratterizzazione meccanica dei materiali e prove di carico sulla struttura di copertura del Padiglione V Torino Esposizioni," Politecnico di Torino, Torino, 2019.

[35] Laboratorio di Dinamica e Sismica , "Relazione sulle prove di caratterizzazione dinamica del Padiglione Morandi di Torino Esposizioni," Politecnico di Torino, Torino, 2019.

[36] U. E. 12504-1:2009, "Testing on concrete in structures – Part 1: Cored specimens – Taking, examining and testing in compression, as amended and supplemented," European Standards, 2009.

[37] U. E. 12390-3:2009, "Testing hardened concrete – Part 3: Compressive strength of test specimens, as amended and supplemented," European Standards, 2009.

[38] R. Ceravolo, G. Coletta, E. Lenticchia, D. Minervini and A. Quattrone, "Dynamic investigation on the health state and seismic vulnerability of Morandi's Pavilion V of Turin Exhibition Center," in *Proceedings of the IABSE Symposium on Synergy of Culture and Civil Engineering - History and Challanges*, Wroclaw, Poland, 2020.

[39] E. Lenticchia, C. R. and M. Chiorino, "Damage scenario-driven strategies for the seismic monitoring of XX century spatial structures with application to Pier Luigi Nervi's Turin Exhibition Centre," *Engineering Structures*, vol. 37, pp. 256-267, 2017.

[40] P. Van Overschee and B. L. De Moor, Subspace identification for linear systems: Theory-Implementation-Applications, Springer Science & Business Media, 2012.

[41] R. Ceravolo and G. Abbiati, "Time domain identification of structures: comparative analysis of output-only methods," *Journal of Engineering Mechanics*, vol. 139, no. 4, pp. 537-544, 2013.

[42] M. L. Pecorelli, R. Ceravolo and R. Epicoco, "An automatic modal identification procedure for the permanent dynamic monitoring of the sanctuary of Vicoforte," *International Journal of Architectural Heritage*, 2018.

[43] ACI201.2R-08, "Guide to Durable Concrete," *ACI Committee 201* , 2008.

[44] Ministero delle Infrastrutture e dei Trasporti, "Nuove Norme Tecniche per le Costruzioni," Gazzetta Ufficiale, Serie generale n. 42 del 20 febbraio 2018, 2018.

[45] CEN, EUROCODE 2, Design of concrete structures, as amended and supplemented, European Standard EN, 2004.

[46] MASTRLAB, "Certificates from the materials testing laboratory at the Politecnico di Torino (1959) Compressive Tests on Concrete, Archive certificate number 6304,6891,7456,7649,7853,8015,8267," Politecnico di Torino - DISEG, Torino, 1959.

[47] Joint Committee on Structural Safety, "Probabilistic assessment of existing structures - JCSS Report," RILEM Publ., 2001.

[48] O. Ditlevsen and H. O. Madsen, Structural reliability methods, New York: Wiley, 1996.

[49] Gazzetta Ufficiale del Regno d'Italia, "Regio Decreto n.2229 - Norme per l'esecuzione delle opere in conglomerato cementizio semplice od armato," 1939.

[50] CEN, "EUROCODE, Basis of structural design, as amended and supplemented," European Standard EN, 1990.

[51] ANSYS.Inc, ANSYS Mechanical APDL. Theory reference. Release15, 2013.

[52] R. Ceravolo, E. Lenticchia, G. Miraglia, V. Oliva and L. Scussolini, "Modal Identification of Structures with Interacting Diaphragms," *Applied Sciences, 12(8), 4030,* 2022.

[53] R. Ceravolo, G. De Lucia, G. Miraglia and M. L. Pecorelli, "Thermoelastic finite element model updating with application to monumental buildings," *Computer-Aided Civil and Infrastructure Engineering,* vol. 35, no. 6, pp. 628-642, 2020.

[54] M. A. Chiorino, "Time dependent effects in concrete structures, draft: suggested revision with contributions by Sassone M," *ACI Committee 209 Creep and Shrinkage of Concrete,* 2008.